Proceedings of the
Annual Stability Conference
Structural Stability Research Council
San Antonio, Texas, March 19-22, 2024

A Refined In-Plane Girder Stiffness Expression for Straight I-Shaped Girder Systems Utilizing Torsional Beam Bracing

David J. Fish[1], Aidan Bjelland[2], Todd A. Helwig[3], Michael D. Engelhardt[4]

Abstract

System and member stability are both major concerns during erection and construction of steel bridges. However, the system buckling limit state is often most critical in relatively narrow girder systems. Member stability is usually controlled by the resistance to conventional lateral-torsional buckling (LTB), which is improved by reducing the unbraced length of the girders with the use of bracing. The most common form of bracing in steel bridges are cross-frames which are categorized as torsional bracing since these braces restrain twist of the girder cross-section. An effective brace must not only provide adequate strength but must also meet certain stiffness requirements. The torsional bracing system stiffness is a function of several components including the stiffness of the braces, the number of in-line braces, cross-sectional distortion, as well as the in-plane stiffness of the girder system. Currently, the bracing design provisions of the AISC Specification do not account for the in-plane girder stiffness, however this stiffness component can dominate the behavior of narrow girder units and may lead to inadequate bracing if it is neglected. This paper presents the verification of a design expression which considers the in-plane stiffness of all girders within a system. The work focuses on the warping rigidity of multi-girder systems, the cumulative stiffness effects of multiple in-line braces, appropriate discretization of a distributed in-plane girder stiffness and extends findings from previous investigations that have targeted the system-buckling mode of narrow girder units.

1. Introduction

Straight I-shaped girders are often utilized in structural steel systems, as they offer efficiency and economy in multiple applications. However, the high strength-to-weight ratio of steel often leads to relatively slender elements, requiring thoughtful considerations of stability limit states. This is particularly true during construction phases when all loading is supported by the non-composite steel sections. The critical limit state under these construction conditions is commonly lateral-torsional buckling (LTB), which is a limit state that involves lateral movement of the compression elements accompanied by a twist of the overall section. This limit state can control at either the individual girder or system level.

[1] Design Engineer, Texas Department of Transportation, <david.fish@txdot.gov>
[2] Graduate Research Assistant, University of Texas at Austin, <aidandrewbjelland@gmail.com>
[3] Jewel McAlister Smith Professorship, University of Texas at Austin, <thelwig@mail.utexas.edu>
[4] Adnan Abou-Ayyash Centennial Professorship, University of Texas at Austin, <mde@mail.utexas.edu>

At the girder level (conventional LTB), the LTB behavior can be improved by reducing the girder's unbraced length. Adequate beam bracing can be achieved by either restraining lateral displacement of the critical compression flange (lateral bracing), or by controlling twist of the girder section (torsional bracing). After a composite deck has been poured and cured, it generally provides both lateral and torsional restraint to all girders. As a result, conventional LTB is not usually a concern in the completed structure. For the construction condition, torsional braces (such as cross-frames or plate diaphragms) are typically employed to serve as stability braces, which enhance the conventional LTB resistance of the individual girders by reducing the girder's unbraced length. However, at the system (or global) level, LTB resistance is primarily a function of the width of the girder system and the provided end warping restraint. Because of this, the number and spacing of intermediate brace points does little to increase the system LTB resistance. Therefore, it is important to ensure that there is adequate system stiffness to provide stability at both the girder and system levels. It is of note that though the system buckling mode failure is most prevalent in bridge systems, it can also control narrow flexural member systems in building applications.

Though effective bracing must provide both adequate stiffness and strength (Winter, 1960), this paper focuses on the requirements for system stiffness. The stiffness of torsional bracing systems is a function of the stiffness of the brace, cross-sectional distortion stiffness, as well as the in-plane stiffness of the girders. Though the in-plane girder stiffness component is not currently accounted for in the AISC specification, recently approved ballot items will account for it in the AASHTO Bridge Design Specification. This stiffness component can dominate the behavior of narrow girder systems and may lead to inadequate bracing if not considered. This is because the in-plane stiffness competent acts at the system level and therefore plays a large role in the system's ability to resist global lateral-torsional buckling.

An in-plane girder stiffness expression was developed in the early 1990's (Helwig, Yura and Frank, 1993). This expression was derived for a twin-girder system which had a single intermediate torsional brace at mid-span. This is the in-plane girders stiffness expression that has been adopted into the AASHTO Bridge Design Specification 10th Edition (2024). However, recent design experiences utilizing this expression suggested that there are common cases in which the provided in-plane girder stiffness is over-predicted when compared to finite element analysis (FEA) solutions. In response to these experiences, and because in-plane girder stiffness can be the limiting factor in girder system stability analyses, Fish (2021) developed a new in-plane girder stiffness expression that accounts for the effect of multiple intermediate cross-frames and girders. The refined expression was not considered for inclusion into AASHTO 2024 because the expression had not been suitably validated with FEA results, which is the purpose of the work documented in this paper. Background information on torsional beam bracing systems, including current design methodologies and the system lateral-torsional buckling mode is presented in the next section.

2. Background

While the conventional lateral-torsional buckling (LTB) resistance can be improved by adjusting girder proportions, the most efficient means of increasing in individual girder's buckling resistance is to reduce the distance between bracing locations, otherwise known as the girder's unbraced length. However, for the system LTB mode, the girder's unbraced length is the entire span and is therefore not affected by the number of intermediate braces.

Conventional LTB is a failure mode that generally consists of a lateral translation of the section accompanied by a twist of the girder cross-section. With suitable bracing, lateral torsional buckling generally occurs within the unbraced length. Timoshenko and Gere (1961) derived the following exact elastic buckling solution for a simply supported, doubly symmetric section, accounting for both St. Venant and warping torsional stiffnesses, which was for the case of uniform moment loading and unrestrained warping at the ends of the unbraced length shown in Eq. 1:

$$M_o = \frac{\pi}{L_b}\sqrt{EI_yGJ + \frac{\pi^2 E^2 C_w I_y}{L_b^2}} \tag{1}$$

where E is the modulus of elasticity, I_y is the weak-axis moment of inertia, L_b is the unbraced length, G is the shear modulus of elasticity, J is the torsional constant, and C_w is the torsional warping constant, as estimated by Eq. 2:

$$C_w = \frac{I_y h_0^2}{4} \tag{2}$$

where h_o is the distance between flange centroids.

Considering the two terms under the radical in Eq. 1, the first is the St. Venant torsional stiffness and is related to the uniform torsional resistance of the section. The second term is related to warping stiffness as well as to the non-uniform torsional stiffness. In the original derivation of Eq. 1, Timoshenko stated that both twist and lateral deformation were restrained at the brace points; however, only the boundary condition of zero twist was enforced in the derivation. Therefore, solely preventing twist of the cross-section results in effective bracing against LTB.

Taylor and Ojalvo (1966) quantified the buckling capacity of a doubly symmetric beam with continuous torsional bracing subjected to uniform moment loading, thereby relating the girder buckling capacity to the stiffness of the brace. This expression is shown in Eq. 3:

$$M_{cr} = \sqrt{M_o^2 + \bar{\beta}_T EI_y} \tag{3}$$

where $\bar{\beta}_T$ is the total distributed torsional brace stiffness (units of moment/radian/unit length).

System LTB occurs when a multi-girder system which is interlinked by braces, such as cross-frames, buckles as a unit (Fig. 1) in a half-sine curve shape. This mode often becomes more critical than conventional LTB (buckling between brace points) in narrow girder systems with small *w/L* ratios; where *w* is the distance between exterior girders and *L* is the span length.

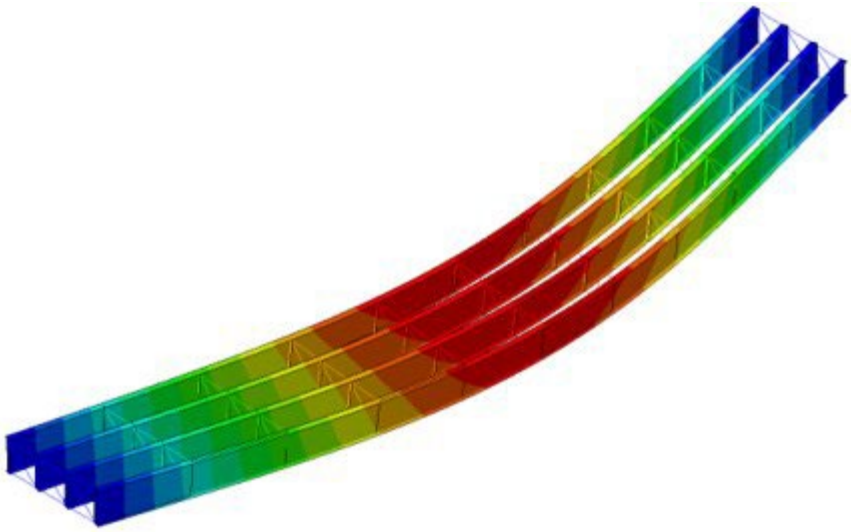

Fig. 1 System Buckling Mode.

Yura et al. (2008) developed the following expression for the elastic global buckling resistance of a doubly symmetric twin I-girder system:

$$M_{g,2008} = \frac{2\pi}{L}\sqrt{EI_y GJ + \frac{\pi^2 E^2 I_y}{4L^2}\left(I_y h_o^2 + I_x s^2\right)} \tag{4}$$

where I_x is the strong-axis moment of inertia, s is the girder spacing and all other variables are as previously defined. All section properties in Eq. 4 (I_x, I_y, J, h_o) are those for a single girder.

When utilizing girders with typical proportions, the St. Venant term in Eq. 4 does not significantly impact the behavior. Neglecting this term and accounting for singly symmetric girders, Yura et al. (2008) produced the simplified expression shown in Eq. 5, which gives the simplified buckling moment capacity for one of the girders in a twin-girder system:

$$M_{gs,2008} = \frac{\pi^2 sE}{n_g L^2}\sqrt{I_{eff} I_x} \tag{5}$$

where n_g is the number of girders in the system and I_{eff} is the effective weak-axis moment of inertia of a singly symmetric girder (Yura, 2001).

Han and Helwig (2020) modified Eq. 5 in order to account for moment gradient, and multiple girders within the system producing the expression shown in Eq. 6:

$$M_{gs,2020} = C_{bs}\frac{\pi^2 (n_g - 1) sE}{n_g L^2}\sqrt{I_{eff} I_x} \tag{6}$$

where C_{bs} is the system level moment gradient factor and all other variables are as previously defined.

As stated previously, Eqs. 4, 5, and 6 are all based on two-girder systems. Additionally, the current AASHTO (2020) provisions allow Eq. 6 to only be used for systems of four girders or less. Since system LTB can control in bridges with more than four girders, Fish (2021) developed a system buckling capacity expression that accounts for any number of girders as shown in Eq. 7:

$$M_{g,2021} = \frac{\pi}{L}\sqrt{EI_yGJ + \frac{\pi^2 E^2 I_y}{L^2}\left(\frac{I_y h_o^2}{4} + \frac{I_x s^2 \alpha_x}{2 n_g}\right)} \tag{7}$$

Eq. 7 can be simplified using the same assumptions as those used for Eq. 5, leading to Eq. 8:

$$M_{gs,2021} = \frac{\pi^2 sE}{L^2}\sqrt{I_y I_x \left(\frac{\alpha_x}{2n_g}\right)} \tag{8}$$

Eqs. 7 and 8 represent an individual girder's global bucking moment capacity and as such, multiplying either expression by the number of girders in the system (n_g) will result in the buckling capacity of the entire system. Additionally, these two equations were derived assuming the same prismatic section was used for each girder. For situations in which non-prismatic and/or non-uniform girder sections are utilized, it is recommended that the length-weighted average approach proposed by Reichenbach et al. (2020) be used to determine the girder section properties. The α_x term in Eqs. 7 and 8 is referred to as the vertical system warping stiffness factor and is akin to the warping stiffness constant (C_w). It is determined by Eq. 9:

$$\alpha_x = \sum\left(n_g - i\right)^2 \tag{9}$$

where the index (i) represents each odd number that is less than n_g as illustrated in Fig. 2.

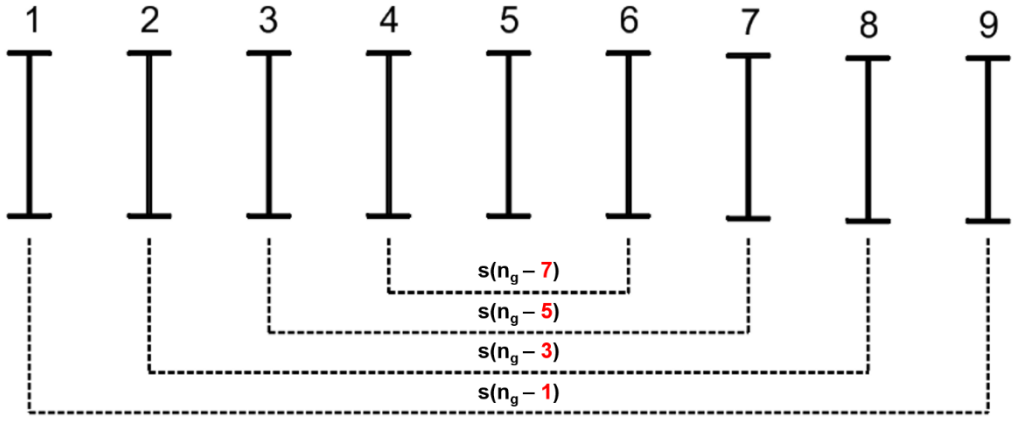

Fig. 2 Vertical system warping stiffness factor indices for a nine-girder system.

Several vertical system warping stiffness factors are provided in Table 1.

Table 1. Vertical System Warping Stiffness Factors (α_x).

Number of Girders[1]	Associated Values of i	α_x
2	1	1
3	1	4
4	1,3	10
5	1,3	20
6	1,3,5	35
…	…	…
9	1,3,5,7	120

1. Eq. 9 can be used to determine warping stiffness factors for systems with other numbers of girders.

With the system (global) buckling capacity of a multi-girder system developed (Eq. 7), an expression to define the total system torsional brace stiffness ($\bar{\beta}_T$) was found by setting Eqs. 3 and 7 equal to one another and simplifying algebraically. The resulting stiffness expression represents the minimum (ideal) system stiffness necessary for global stability. A brief background of the torsional brace stiffness requirements is provided below.

Winter (1960) developed a model that demonstrated a simple means by which the ideal stiffness requirements for lateral bracing systems can be determined. The ideal stiffness is the minimum stiffness required that allows a member to reach a load level corresponding to buckling between the brace points. Winter's model also demonstrated the impact of imperfections on the buckling behavior, and that a stiffness larger than the ideal stiffness was necessary to control member deformations and brace forces. As a result, most bracing provisions currently recommend using twice the ideal stiffness. Liu and Helwig (2020) showed that requiring three times the ideal stiffness provides better control of brace forces for torsional beam bracing systems when the critical shape imperfection involves a lateral sweep of the compression flange while the tension flange remains straight. This imperfection shape was found to be the worst case for beams (Wang and Helwig, 2005); however, if the brace is sufficiently deep, the critical initial imperfection shape is better represented by a pure sweep of the section and providing twice the ideal stiffness is appropriate (Han and Helwig, 2020).

The torsional beam bracing provisions in the upcoming AASHTO Bridge Design Specification 10th Edition (2024) provide stiffness and strength requirements that are a function of the design moment, M_u. This design moment is the load that a braced girder is subjected to at the stage in question. As noted earlier, the critical stage for LTB stability is generally during construction, particularly during pouring of the concrete deck. Therefore, M_u will typically be the maximum factored construction moment during casting of the slab. Assuming that the braces being used are at least 80 percent of the depth of the girder, the system stiffness requirement in the approved AASHTO provisions is given by the following expression:

$$(\beta_T)_{req} = \frac{2.4L}{\phi_{sb} n E I_{yeff}} \left(\frac{M_u}{C_b}\right)^2 \tag{10}$$

where ϕ_{sb} is the stability bracing resistance factor (0.8), C_b is the moment gradient factor within the critical unbraced beam or girder, and n is the number of intermediate cross-frames.

The provided system stiffness (which must be equal to or greater than the required system stiffness of Eq. 10) is a function of several bracing components: stiffness of the brace (β_{br}); cross-sectional distortion stiffness (β_{sec}); and the in-plane girder stiffness (β_g). Like many bracing systems, torsional beam bracing follows the fundamental equation for springs in series, such that the torsional system stiffness is given by the following expression:

$$\frac{1}{\beta_T} = \frac{1}{\beta_{br}} + \frac{1}{\beta_g} + \frac{1}{\beta_{sec}} \tag{11}$$

There are a number of sources that discuss the background of an individual brace's stiffness and the effects of cross-sectional distortion (AISC 2016, Yura 2001). The focus of the research documented in this paper is on the in-plane girder stiffness component, which is discussed in more detail next.

When multiple girders are connected by bracing, such that they act as a unit, the in-plane (i.e., major axis) flexural stiffness of the individual girders contribute to the overall stiffness of the torsional bracing system. As shown in Fig. 3, when the girders are subjected to a twist, the internal moment that is subsequently developed in the cross-frame is equilibrated by vertical shear forces acting at the ends of the brace. The vertical forces on the adjacent girders cause one girder to deflect upwards and the other to deflect downwards leading to a rigid body rotation. These deformations reduce the effectiveness of the bracing system. With a wider system, this displacement is reduced, as demonstrated by the four-girder system shown in the figure.

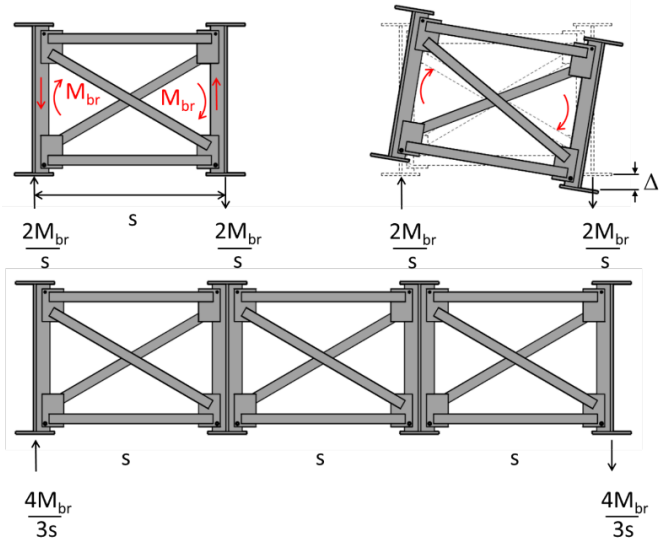

Fig. 3 In-Plane Girder Stiffness

The behavior illustrated in Fig. 3 was initially quantified by Helwig, Yura and Frank (1993) for a two-girder system with a single torsional brace at mid-span and was expanded to multiple-girder systems by Yura (2001) as shown in Eq. 12:

$$\beta_{g,1993} = \frac{24(n_g - 1)^2 s^2 EI_x}{n_g L^3} \tag{12}$$

Considering Eq. 11, if β_g is less than the required β_T, full bracing cannot be achieved, regardless of the stiffness of the brace that is utilized. From a buckling perspective, if the in-plane stiffness of the girder is insufficient, the system mode will generally control over buckling between the brace points. Because the system mode of buckling is closely tied to the in-plane stiffness requirements, Fish (2021) utilized a system mode approach to derive a more accurate expression which accounts for multiple girders within the system cross-section. This expression is shown in Eq. 13:

$$\bar{\beta}_g = \frac{\pi^4 E I_x s^2 \alpha_x}{2 n_g L^4} \tag{13}$$

Eq. 13 was derived directly from Eqs. 3 and 7, thereby accounting for the relationship between the system buckling capacity and in-plane girder stiffness. The initial derivation of Eq. 13 resulted in the in-plane girder stiffness being presented as a distributed stiffness having units of k-in/rad/in. However, in order to be utilized in bracing design provisions, the in-plane girder stiffness must be discretized and attributed to each torsional brace along the girder's length. The appropriate discretization of the in-plane girder stiffness was studied and is discussed in a later section.

3. Parametric Studies

FEA parametric studies were conducted to evaluate the validity of the proposed in-plane girder stiffness expression. Two separate investigations were conducted focusing on A) the effective bracing as a function of number of cross-frames in a given line, and B) a study focused on the in-plane girder stiffness. Investigation A related to the effective bracing was divided into 2 phases. The first phase consisted of conducting analyses to identify the ideal system stiffness for each girder system, which was then used in the second phase to establish the effective brace stiffness of a given line of cross-frames with each girder system. Investigation B was focused on determining the in-plane girder stiffness from the FEA studies as a function of various girder geometries. The in-plane girder stiffness, as predicted by FEA, was used to verify the predictive capabilities of the proposed expression given in Eq. 13. The overall parametric study methodology; modeling assumptions; determination of the ideal system, effective brace and in-plane girder stiffnesses; and the comparison results are presented in the following sections.

3.1 Methodology Rationale

For the purposes of evaluating the accuracy of the derived expression in Eq. 13, the resulting in-plane girder stiffness from the FEA needed to be determined. However, as shown in Eq. 11, accurate estimates of all the system components are necessary in order to make direct comparisons between Eq. 13 and the in-plane girder stiffness of a given system as obtained from finite element analyses ($\beta_{g,FEA}$). Therefore, the study methodology was ultimately concerned with isolating the in-plane girder stiffness from the other stiffness terms: brace stiffness and cross-sectional distortion stiffness. Considering Eq. 11, to isolate in-plane girder stiffness, the three other terms must be known. The treatment of brace and cross-sectional distortion stiffness values is relatively straight forward and are addressed below. However, the ideal torsional system stiffness ($\beta_{T,ideal}$), which is the unique minimum system stiffness required to achieve buckling between the brace points, must be determined by analysis.

As demonstrated by the methodology utilized in Liu and Helwig (2020) and Fish (2021), a given term can be isolated by creating a significant disparity between the components; such that the secondary components are large enough numerically to be considered negligible, which therefore only leaves the focal stiffness component. By utilizing full depth cross-frames, the cross-sectional stiffness (β_{sec}) component can be considered negligible for use in Eq. 11 (AASHTO 2024), thereby leaving only β_g and β_{br}. With β_{sec} removed from consideration, Fig. 4 illustrates the relationship the remaining stiffness components have to the total ideal system stiffness. As shown, an individual stiffness component does not need to be numerically infinite to be reasonably assumed to act as infinitely stiff.

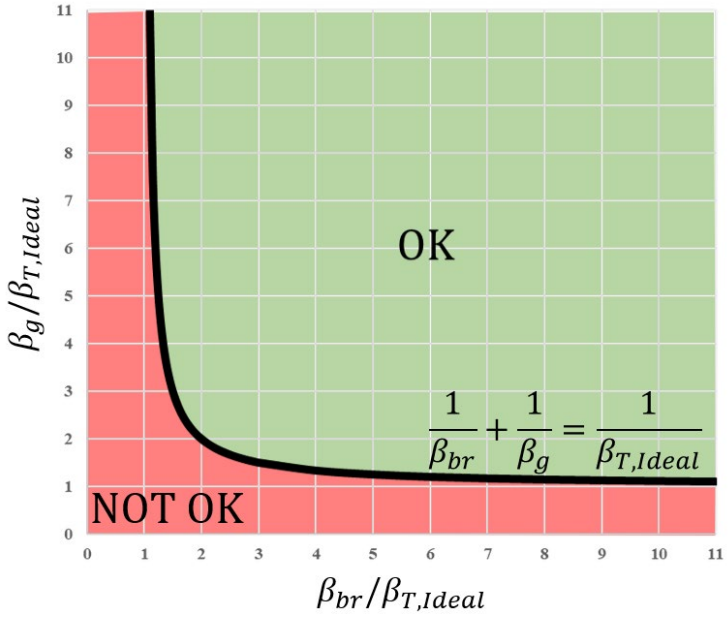

Fig. 4 Relationship between stiffness components relative to the ideal torsional brace stiffness of the system.

With infinite cross-sectional stiffness, the individual brace stiffness (β_{br}) and in-plane girder stiffness (β_g) are the only two remaining independent unknowns, and two options exist to isolate one or the other:

1. Increase the stiffness of the brace (by way of increasing the area of the brace members) such that β_{br} can be eliminated, thereby isolating β_g.
2. Increase the w/L ratio such that β_g can be eliminated, thereby isolating β_{br}.

Though the eventual goal is to isolate the in-plane girder stiffness, $\beta_{T,ideal}$ must first be identified. This was accomplished by having both cross-sectional distortion and in-plane girder stiffness values tend towards infinity, thereby isolating the brace stiffness component. With β_{br} as the only remaining unknown, the minimum brace stiffness required to achieve buckling between the brace points can be taken as equivalent to the ideal torsional system stiffness. For a given girder cross-section, this value can be obtained by considering a relatively wide twin-girder system and is illustrated in Fig. 5.

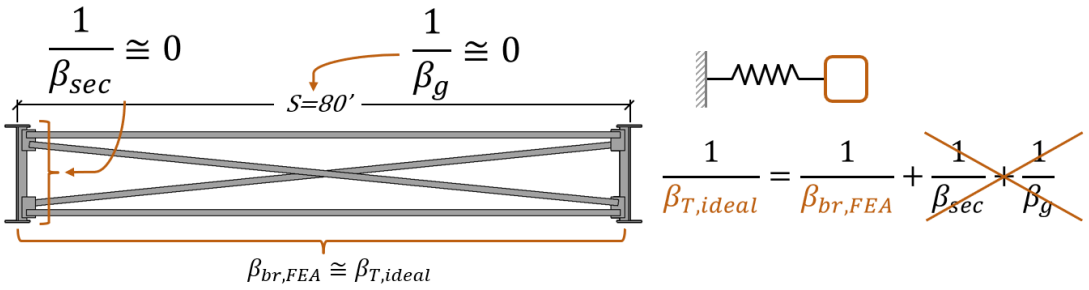

Fig. 5 Idealized system isolating the effects of a single stiffness component such that $\beta_{T,ideal}$ can be obtained.

The concept of eliminating β_g by widening the system to extreme levels was first used by Liu and Helwig (2020). Though the stated reasoning for using such a wide system was to avoid the system buckling mode, due to the relationship between the in-plane girder stiffness and system buckling described previously, an increase in system bucking capacity leads directly to an increase in β_g. Therefore, this concept of increasing β_g to the point that it can be considered infinite was utilized and expanded upon in this study.

3.2 Model Properties

The finite element models utilized a combination of shell and truss elements as shown in Fig. 6. The girders and stiffeners were meshed with S4 linear shell elements whereas bracing members were comprised of single T3D2 linear truss elements. The mesh density for the shell elements was selected with an aspect ratio for the shells close to unity in Abaqus (2022). While perfect unity throughout was not possible, most aspect ratios varied between approximately 2/3 and 3/2. Additionally, stiffener elements were only attached to the web of the girders to minimize warping restraint that the plate elements might provide. Bracing members were attached at the web-flange juncture nodes.

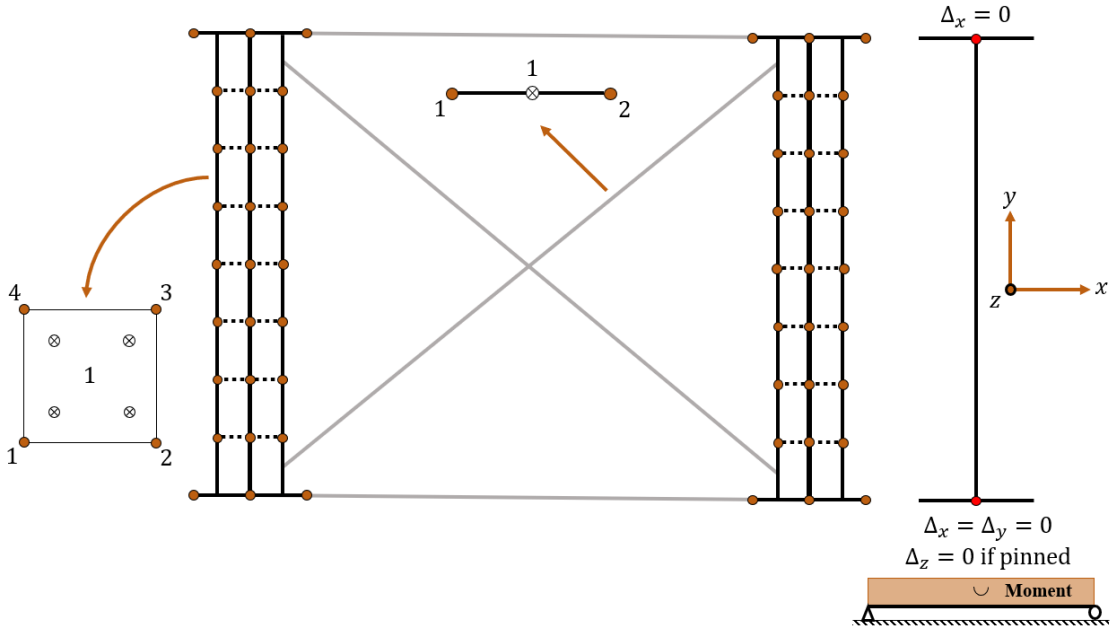

Fig. 6 Illustration demonstrating model elements, meshing, boundary conditions, and applied load.

To ensure consistent results when compared to hand calculations, the meshed web depth was set to match the depth of the section. The thickness property applied to shell elements was centrally distributed for the web and stiffener elements but shifted vertically for the flange elements to prevent mass overlap.

Support boundary conditions mimic a simply-supported system and restrain lateral movement of both top and bottom flanges. Restraining lateral movement of the top and bottom flanges leads to the no-twist boundary condition assumed in the derivation of the buckling expressions. Another assumption employed in these derivations was that warping was unrestrained at the supports which was also accounted for in the models. A force couple oriented along the longitudinal axis of the girder and placed at the web-flange juncture nodes at each support was used to mimic a constant uniform moment loading on the girders.

3.3 Determination of the Ideal Torsional System Stiffness ($\beta_{T,ideal}$)

As mentioned previously, the assessment of β_g relies on an accurate determination of $\beta_{T,ideal}$. To that end, a parametric study employing the idealized system method illustrated in Fig. 5 was performed utilizing the system geometry parameters shown in Table 2.

Table 2. System geometry parameters utilized in ideal stiffness parametric study.

Bridge Parameters	Value Range
Girder Spacing	[80’]
Number of Girders	[2]
Number of Cross-frame Lines	[1, 2, 3]
Unbraced Length	[40’]

The girder sections tested are shown in Fig. 7.

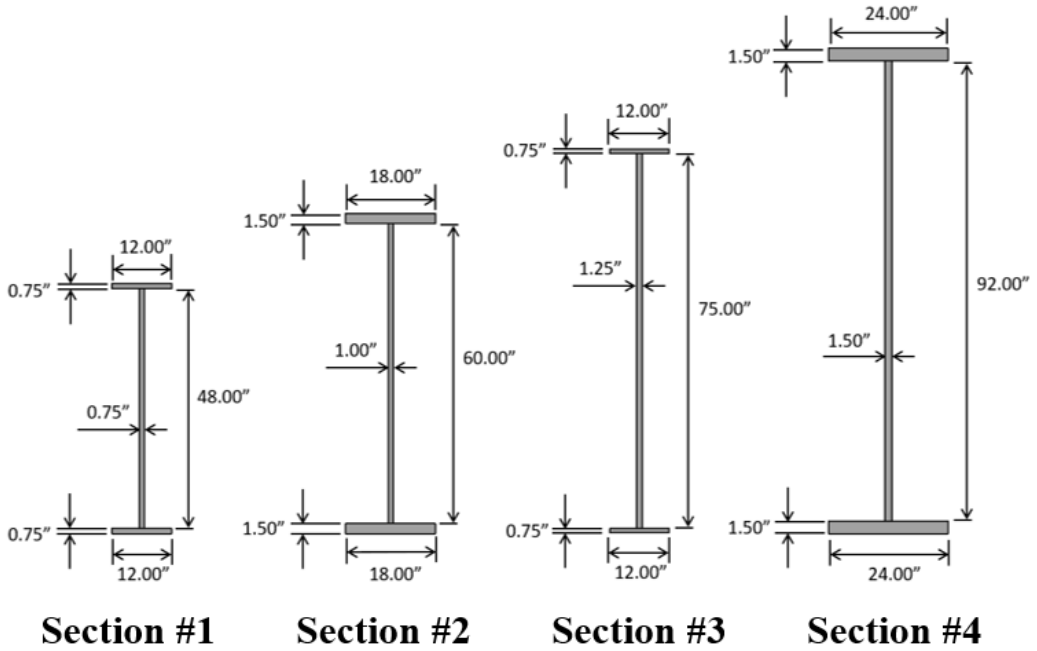

Fig. 7 Girder sections used for parametric studies.

3.3 Determination of an Effective Brace Stiffness ($\beta_{br,eff}$)

Brace stiffness expressions typically only represent the stiffness of a single brace between two adjacent girders. However, during the course of the ideal torsional system stiffness parametric study, it was determined that there is an appreciable, and beneficial, effect when multiple in-line cross-frames are present (Fish et al., 2024). For example, with a twin girder system, at each brace location along the girder length a single brace restrains the girders (0.5 brace/girder). If three girders are utilized, there are two braces restraining three girders (0.67 brace/girder). As more girders are added, the number of braces tend to approach one brace per girder. Therefore, the individual brace stiffness required to achieve buckling between the brace points decreases as more girders (and therefore cross-frames) are added. Because this behavior was determined to act in a predictable way, an expression was developed that could be used as an adjustment factor to be applied to the basic brace stiffness expression. The brace stiffness adjustment factor (C_{nc}) can be determined by Eq.14:

$$C_{nc} = 1 + \frac{n_g - 2}{n_g + 1.75} \tag{14}$$

Multiplying the individual brace stiffness (β_{br}) by the brace stiffness adjustment factor (C_{nc}) produces an effective brace stiffness ($\beta_{br,eff}$), which more accurately predicts the brace stiffness of a given cross-frame line. Because the resulting brace stiffness represents the effective brace stiffness – a more accurate representation of the in-plane girder stiffness of the associated system can therefore be determined. This process is outlined in the next section.

3.4 Determination of the In-Plane Girder Stiffness (β_g)

For the $\beta_{T,ideal}$ study discussed previously, the in-plane girder stiffness component was eliminated by using an extremely wide system (Fig. 5). In order to determine the in-plane girder stiffness, as predicted by FEA, β_g was reintroduced to the model. This was accomplished by reducing the girder spacing such that the *w/L* ratio would be decreased, causing β_g to have a discernable impact on the system solution.

The minimum brace stiffness required to buckle between brace points was determined for several girder systems using the parameters defined in Table 3.

Table 3. System parameters tested in the β_g verification study.

Bridge Parameters	Value Range
Girder Spacing	$[8', 10', 12']$
Number of Girders	$[2,\ 3,\ 4,\ 5]$
Number of Cross-frame Lines	$[1,\ 2,\ 3,\ 5]$
Unbraced Length	$[20', 40']$
Girder Sections	$[\#1, \#2, \#3, \#4]$

For a given girder cross-section and brace spacing, the ideal torsional brace stiffness, $\beta_{T,ideal}$, is a constant. Since $\beta_{T,ideal}$ is known from the previous analyses, and $\beta_{br,eff}$ was determined from the first investigation considering the parameters listed in Table 3, $\beta_{g,FEA}$ was calculated based upon Eq. 15:

$$\beta_{g,FEA} = \frac{1}{\frac{1}{\beta_{T,ideal}} - \frac{1}{\beta_{br,eff}}} \tag{15}$$

The stiffness described by Eq. 15 represents the in-plane girder stiffness attributed to each brace line in the system. In order to achieve a direct comparison between the FEA results and the proposed in-plane girder expression, an appropriate discretization of Eq. 13 was necessary. The results of that investigation are presented next.

3.5 Discretization and Evaluation of the Proposed In-Plane Girder Stiffness Expression

The in-plane stiffness component derived from the system buckling expressions discussed previously resulted in a "continuous" stiffness formulation. For consideration in torsional bracing problems, a method of discretization is necessary to obtain a stiffness component for use with a given bracing line. Two discretization options of the $\bar{\beta}_g$ expression were investigated: L/n and $L/(n+1)$, as shown in Eqs. 16 and 17:

$$\beta_{g,L/n} = \frac{\pi^4 E I_x s^2 \alpha_x}{2 n_g L^4 n} \tag{16}$$

$$\beta_{g,L/(n+1)} = \frac{\pi^4 E I_x s^2 \alpha_x}{2 n_g L^3 (n+1)} \tag{17}$$

$\beta_{g,FEA}$ was calculated using the FEA determined minimum brace stiffness required for buckling between the brace points and is therefore highly dependent upon the accuracy of that brace stiffness. However, due to the nature of the springs in series expression, slight variations in the accuracy of the brace stiffness can lead to large variations of the in-plane girder stiffness component. As a result, it was determined that the most useful verification approach would be to compare the effect of the in-plane girder stiffness on the overall system stiffness ($\beta_{T,eq}$) represented by Eq. 18 to the known ideal system stiffness ($\beta_{T,ideal}$) represented by Eq. 19:

$$\frac{1}{\beta_{T,eq}} = \frac{1}{\beta_{br,eff}} + \frac{1}{\beta_{g,eq}} \tag{18}$$

$$\frac{1}{\beta_{T,ideal}} = \frac{1}{\beta_{br,eff}} + \frac{1}{\beta_{g,FEA}} \tag{19}$$

Fig. 8 compares the overall system stiffness predicted when using Eqs. 16 and 17 in Eq. 18 to that of the system stiffness determined by FEA.

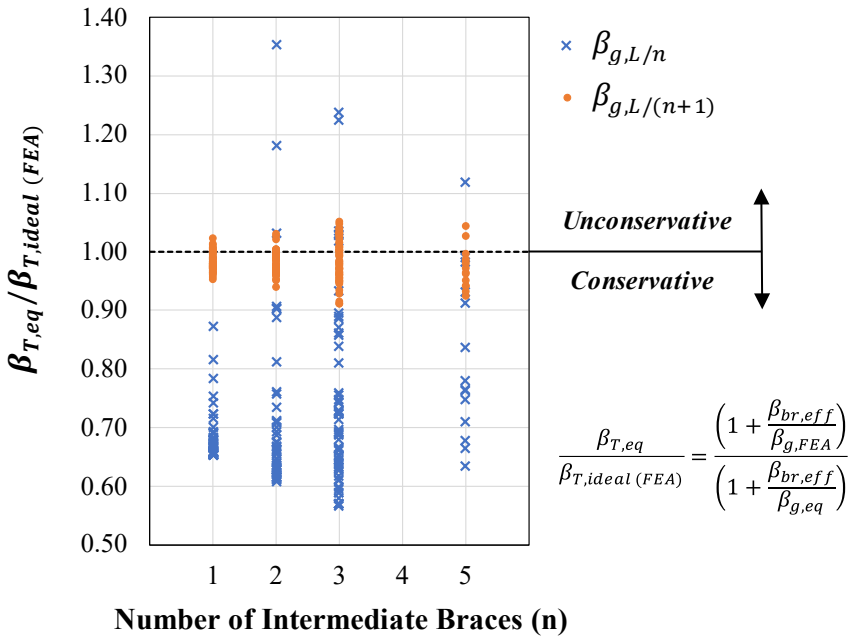

Fig. 8 Comparison of the $\beta_{g,L/n}$ and $\beta_{g,L/(n+1)}$ discretization options.

The results depicted in Fig. 8 suggest that the L/n discretization is typically overly conservative and that $L/(n+1)$ more accurately represents the system stiffness. As a result, the proposed in-plane girder stiffness expression for the case of uniform moment and accounting for discretization is shown in Eq. 20:

$$\beta_{g,2023} = \frac{\pi^4 E I_x s^2 \alpha_x}{2 n_g L^3 (n+1)} \tag{20}$$

The true improvement of the in-plane girder stiffness expression can be best seen by comparing the new expression to the original 1993 equation. Fig. 9 demonstrates the scatter of the original 1993 expression from the wide range of bridges tested. In contrast, the proposed $\beta_{g,2023}$ expression tightly bounds the data within ~5% of the expected value.

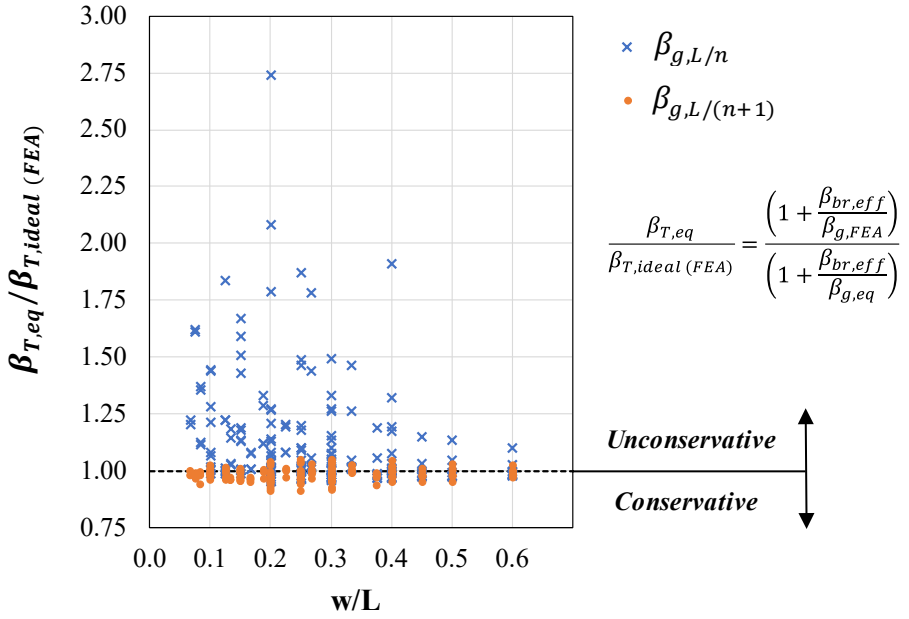

Fig. 9 Comparison of $\beta_{g,1993}$ and $\beta_{g,2023}$ expressions.

These results were invariant when comparing the girder spacing, number of intermediate braces, unbraced length, and cross-section. Minor variance was observed when sorting the data with regard to the number of girders, but the majority of results were still within ~5% of the expression. The reason speculated to have caused this variance is that the methodology becomes hyper-sensitive as β_g approaches an infinitely stiff component. Thus, a wider bridge with more girders may lead the methodology to begin underpredicting the β_T. Overall, the results demonstrate that the new β_g and $\beta_{br,eff}$ expressions are able to accurately capture the stiffnesses produced by FEA for a variety of conventional bridge systems.

4. Conclusions

Due to the limited application (twin-girder systems) and unconservative nature of the 1993 in-plane girder stiffness expression as shown in this paper, adoption of the newly verified in-plane girder stiffness expression is recommended. The proposed expression was shown to produce values within approximately 5% of the values predicted by finite element analysis. It is also recommended that the brace stiffness adjustment factor (C_{nc}) be adopted in order to account for the previously unattributed benefits of multiple in-line cross-frames. However, neglecting the benefit of multiple in-line cross-frames is a conservative approach.

Further research is currently underway determining the effects of system level moment gradient as well as utilizing lateral truss systems and/or deck pour sequencing to produce system-end warping restraint, thereby increasing both the system buckling capacity and in-plane girder stiffness.

References

AASHTO (2020) LRFD Bridge Design Specifications. 9th edn. Washington, DC: American Association of State Highway and Transportation Officials.

AASHTO (2024) LRFD Bridge Design Specifications. 10th edn. Washington, DC: American Association of State Highway and Transportation Officials.

Abaqus Unified FEA (2022). Available at: https://www.3ds.com/products-services/simulia/products/abaqus/.

AISC (2016) Specification for Structural Steel Buildings. Chicago: American Institute of Steel Construction.

Fish, D.J. (2021) Refined Design Expressions for In-Plane Girder Stiffness and System Buckling Capacity. Master's Thesis. University of Texas at Austin.

Fish, D.J. et al. (2024) Torsional Beam Bracing Design for Straight I-Shaped Girder Systems. Unpublished.

Han, L. and Helwig, T. (2020) Elastic Global Lateral-Torsional Buckling of Straight I-Shaped Girder Systems, ASCE Journal of Structural Engineering, 146(No .4), p. (10 pages).

Helwig, T., Yura, J. and Frank, K. (1993) Bracing Forces in Diaphragms and Cross Frames, Structural Stability Research Council Conference "Is Your Structure Suitably Braced?", pp. 129–140.

Liu, Y. and Helwig, T. (2020) Torsional Brace Strength Requirements for Steel I-Girder Systems, Journal of Structural Engineering, 146(1), p. 04019185. Available at: https://doi.org/10.1061/(ASCE)ST.1943-541X.0002482.

Reichenbach, M. et al. (2020) Lateral-Torsional Buckling of Singly Symmetric I-Girders with Stepped Flanges. ASCE Journal of Structural Engineering, 146(10), pp. 04020203-1-15 (15 pages).

Taylor, A.C. and Ojalvo, M. (1966) Torsional Restraint of Lateral Buckling. Journal of the Structural Division, ASCE, ST2, pp. 115–129.

Timoshenko, S. and Gere, J. (1961) Theory of Elastic Stability. New York: McGraw-Hill.

Wang, L. and Helwig, T.A., "Critical Imperfections for Beam Bracing Systems," *ASCE Journal of Structural Engineering,* Vol. 131, No. 6, pp. 933-940, June 2005.

Winter, G. (1960) Lateral Bracing of Columns and Beams. ASCE Transactions, 125, pp. 809–825.

Yura, J.A. (2001) Fundamentals of Beam Bracing. Eng. J.; 11-26

Yura, J.A. et al. (2008) Global Lateral Buckling of I-Shaped Girder Systems. Journal of Structural Engineering, 134(9), pp. 1487–1494.